Output

1. ผลงานตีพิมพ์ในวารสารวิชาการนานาชาติ:

Y. Boonyongmaneerat, K. Saengkiettiyut, S. Saenapitak, and S. Sangsuk, "Effects of WC addition on structure and hardness of electrodeposited Ni-W," *Surface &Coatings Technology*, vol. 203, pp. 3590-4, 2009.

2. การนำผลงานวิจัยไปใช้ประโยชน์

ได้มีการนำผลงานวิจัยไปใช้ประโยชน์ในเชิงวิชาการ กล่าวคือ มีการเผยแพร่งานวิจัยในที่ประชุมวิชาการ และนำความรู้ไปใช้ในการเรียนการสอนนิสิตและนักศึกษา การนำเสนอผลงานวิจัยทำให้ผู้ที่ได้รับความรู้ทราบถึงหลักการและกระบวนการพัฒนาโลหะชุบเคลือบที่มีสมบัติที่เหมาะสมในการใช้งาน ตลอดจนการได้ตระหนักถึงความสำคัญของการผลิตวัสดุด้วยกระบวนการที่เป็นมิตรต่อสิ่งแวดล้อม ในอนาคตผู้วิจัยคาดว่าจะนำองค์ความรู้ที่ได้รับจากงานวิจัยนี้ต่อยอดเป็นงานวิจัยเชิงประยุกต์เพื่อพัฒนาผลิตภัณฑ์โลหะชุบเคลือบที่เป็นประโยชน์ในเชิงพาณิชย์ เพื่อประโยชน์ต่อภาคอุตสาหกรรมโดยตรงต่อไป

Surface & Coatings Technology 203 (2009) 3590–3594

Contents lists available at ScienceDirect

Surface & Coatings Technology

journal homepage: www.elsevier.com/locate/surfcoat

Effects of WC addition on structure and hardness of electrodeposited Ni–W

Yuttanant Boonyongmaneerat *, Kanokwan Saengkiettiyut, Sawalee Saenapitak, Supin Sangsuk

Metallurgy and Materials Science Research Institute, Chulalongkorn University, Bangkok, 10330 Thailand

ARTICLE INFO

Article history:
Received 13 January 2009
Accepted in revised form 17 May 2009
Available online 22 May 2009

Keywords:
Electroplating
Nickel–tungsten alloys
Tungsten carbide
Composite coatings
Structural properties

ABSTRACT

Nickel–tungsten/tungsten carbide composites (Ni–W/WC) are fabricated by co-electrodeposition. Processing parameters including current density, particle content, and particle size are found to influence surface morphology and consequently the apparent hardness of the co-deposits. A cathodic current density below 0.2 A/cm^2 and solid loading between 1 and 2 g/l are essential for providing deposits with non-porous and uniform structure. The use of 0.5 μm tungsten carbide particles and a current density of 0.1 A/cm^2 results in a Ni–W/WC composite of fine and dense nodular structure with hardness of about 10 GPa, exceeding those of nanocrystalline nickel–tungsten alloys and comparable to that of hard chromium coating.

1. Introduction

Co-electrodeposition refers to the electrolytic process by which reduced metal ions together with ceramic or organic particles are deposited on a substrate, forming a composite structure of metal matrix dispersed by the particles. The inert inclusions can potentially enhance the performance of the metals in several ways, such as improvements of hardness, wear resistance, and corrosion properties [1]. Owing to its relatively low operational cost and low processing temperature, the co-electrodeposition technique has been aggressively developed. Examples of the metal/inclusion electrodeposited systems which have been investigated and fabricated successfully include Ni/Al_2O_3 [2,3], Ni/SiO_2 [4,5], Au/diamond [6], Cu/Al_2O_3 [7,8], and Cu/carbon nanotube [9].

Electrodeposited nickel–tungsten (Ni–W) alloys were recently developed as a candidate to replace the environmentally hazardous hexavalent hard chromium coating. By controlling their grain size into the nanocrystalline regime through modification of cathodic current conditions, the hardness of Ni–W alloys can be enhanced from ~1 GPa to as much as ~7 GPa [10]. Nevertheless, it is still inferior to the traditional chromium coating, which exhibits high hardness of ~10 GPa [11,12]. Addition of hard particles to the nanostructured Ni–W alloys could therefore serve as a potential strategy to further improve their hardness. Furthermore, the co-electrodeposition process could benefit in the enhancement of other properties of the alloys, such as wear and corrosion resistances.

While prior works on co-electrodeposition have concentrated on single-phase metal deposits, with emphasis on micro-grain Ni as the base metal [2–5], studies on alloy systems, such as Ni–W, with particle inclusions, and on their structure–property relationships are very limited. B. Han and X. Lu [13], Y. Yao et al. [14], and L. Shi et al. [15] investigated very recently the co-electrodeposition of Ni–W/CeO_2, Ni–W/SiC, and Ni–Co/SiC, respectively. It is found that in general the particle content incorporated in the deposit increases with the current density and solid loading, and that the inclusions help improve the tribological and corrosion properties of the deposits.

Here, we investigated the co-electrodeposition of Ni–W and WC, the latter of which was selected as reinforcing material due to its high hardness, superior wear resistance, and good corrosion properties. The prior work by Z. Abdel Hamid et al. [16] on the co-electrodeposition of Cr and WC, for example, has shown that the incorporation of 50 vol.% WC particles into Cr matrix led to significant reductions of wear rate from 2.6 g/s to 0.5 g/s and corrosion rate from 13 μm/yr to 2 μm/yr. Similarly, K. Van Acker et al. [17] has demonstrated in their laser clad Ni/WC composite study that ~45 vol.% WC reinforce helped improve wear resistance of Ni by more than 200 times. In the present study, the effects of processing parameters in the co-electrodeposition process including current density, WC particle content, and particle size on the structure and hardness of Ni–W/WC deposits were examined. The understanding of the possible deposition mechanism and the relationship between the processing parameters and mechanical property gained from the study would lead to the optimal designs of Ni–W/WC composites.

2. Experimental

The co-electrodeposition of Ni–W and WC was conducted in a plating bath with aqueous bath chemistry: 18 g/l $NiSO_4 \cdot 6H_2O$, 53 g/l $Na_2WO_4 \cdot 2H_2O$, 168 g/l $Na_3C_6H_5O_7 \cdot 2H_2O$, 31 g/l NH_4Cl, 18 g/l NaBr, with the temperature maintained at 75 °C. WC powders with the average particles size of 3 and 0.5 μm (ATI Alldyne, Huntsville AL) (Fig. 1a and b)

* Corresponding author. Tel.: +66 2 218 4243; fax: +66 2 611 7586.
E-mail address: yuttanant.b@chula.ac.th (Y. Boonyongmaneerat).

0257-8972/$ – see front matter © 2009 Elsevier B.V. All rights reserved.
doi:10.1016/j.surfcoat.2009.05.027

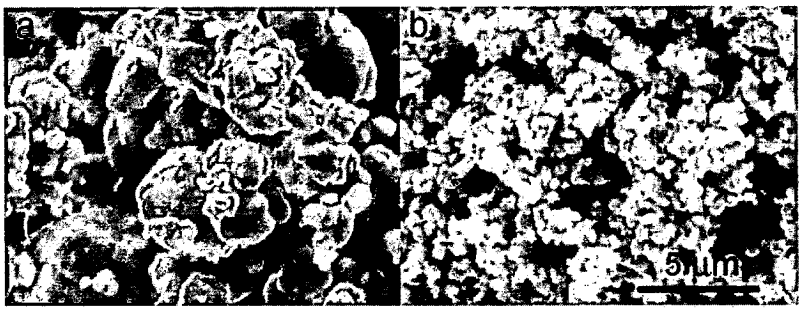

Fig. 1. Tungsten carbide (WC) particles with the average size of (a) 3 μm and (b) 0.5 μm used in the study. They are termed micro and sub-micro WC, respectively. The scale bar is for both parts of the figure.

and solid loading of 0, 0.2, 1, and 2 g/l were used. The pH of the electrolyte was 8.9, and it was unaffected by the WC additions. Copper, polished to a mirror-like finish, and platinum were respectively employed as a cathode and an anode. Prior to plating, a copper substrate (1.0×2.4 cm^2) was activated in 10% H_2SO_4, and the WC-filled electrolyte was sonicated in an ultrasonic bath to assist in particle de-agglomeration. Upon deposition, a direct current of 0.1, 0.15, or 0.2 A/cm^2 was applied to the system that contained micro particles, and 0.1 A/cm^2 was used in the plating baths with sub-micro particles. To suspend WC particles in the solutions, a magnetic bar was continuously rotated at 500 rpm. Since WC incorporations, as investigated in the study, do not significantly affect the cathodic efficiency of the system, the WC content in the coatings was estimated by comparing the weight of the co-deposits and of WC-free specimens processed under the same condition. X-ray diffractrometer (XRD), energy-dispersive spectroscopy (EDS), and scanning electron microscopy (SEM) were employed to characterize the composition and surface morphology of the specimens. Hardness of the materials was assessed using a Vickers micro-indenter with a load of 500 g (Mitutoyo, MVK-H2).

3. Results

Specimens with uniform and intact deposits were obtained in all cases of processing parameters employed, except for the system with 2 g/l of sub-micro WC where some surface cracks were observed in the deposit. The thickness of the coatings ranges from 20 to 40 μm, depending on the current densities used. Furthermore, it was observed that WC addition in the bath did not clearly affect the deposition rate of the alloys. Micrographs, which show surface morphology of the as-deposited specimens, are presented in Figs. 2–5. The specimen that was fabricated with 0.2 g/l of micro particles and a 0.1 A/cm^2 current density is characterized by a matrix that is dispersed by agglomerates of nodules, whose size is much larger than that of WC particles (Fig. 2a). Upon increment of WC content to 1 g/l and 2 g/l in a plating bath, the similar surface morphology is retained, but the nodules in the agglomerates appear smaller at higher particle loadings (Fig. 2b and c).

As the current density was increased to 0.15 A/cm^2 (0.2 g/l micro WC), agglomerates of nodules previously observed are not clearly evidenced, but there presents the second type of nodular surface morphology that is more uniform and finer in size throughout the surface (Fig. 3a). Such meso-scale structure is commonly observed in many electrodeposited materials [10,18], and is noted to be a grain colony – for this Ni–W system, it is a cluster of nanocrystalline grains [19]. Additionally, some large circular nodules also disperse on the surface of the specimen. The increase of particle solid loading to 1 g/l induces the increase of nodular size and the formation of a structure with morphology similar to a pattern of a turtle shell (Fig. 3b). Finally, at 2 g/l of WC, the structure becomes porous and entirely composes of agglomerates of nodules (Fig. 3c).

Increasing the current density further to 0.2 A/cm^2, the specimen with 0.2 g/l micro WC (Fig. 4a) exhibits similar surface morphology to that processed with the same solid loading at 0.15 A/cm^2 (Fig. 3a), except the nodules are generally larger. Furthermore, the number of large nodules appears to increase with the increment of particle solid loading to 1 g/l and 2 g/l (Fig. 4b and c).

When the sub-micro WC particle was employed using a 0.1 A/cm^2 current density, the resulting surface morphology of the specimen with 0.2 g/l WC is comprised of a matrix dispersed by some large circular nodules (Fig. 5a). As the solid loading was increased to 1 g/l, the corresponding structure appears to compose almost entirely of agglomerates of nodules, whose size is much larger than that of the WC particles (Fig. 5b). Similar surface morphology is also observed in the specimen with 2 g/l WC. However, the structure becomes very porous (Fig. 5c).

Fig. 6 shows the content of WC incorporated in the coatings, as a function of solid loading. It is observed that the content of WC generally increases with solid loading, corresponding to what was found in several co-electrodeposited systems [4,8,13]. Furthermore, compared to other specimens, the deposits processed at a relatively high current density of 0.2 A/cm^2 contained relatively low WC content. Metallography performed on the cross-section of some of the co-deposit specimens reveals that WC particles are dispersed in the metal matrix without any adverse reaction along particle/matrix surfaces.

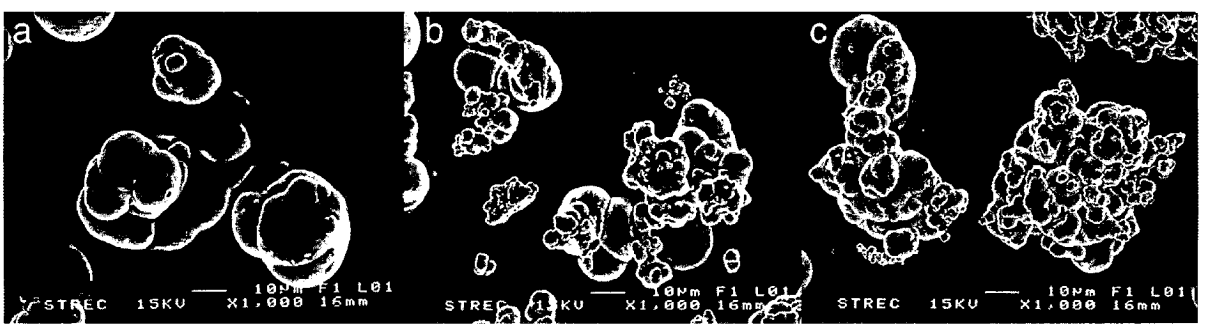

Fig. 2. Surface morphology of Ni–W/micro WC composites processed with a current density of 0.1 A/cm^2 and WC content of (a) 0.2 g/l, (b) 1 g/l, and (c) 2 g/l in a plating bath.

Fig. 3. Surface morphology of Ni–W/micro WC composites processed with a current density of 0.15 A/cm^2 and WC content of (a) 0.2 g/l, (b) 1 g/l, and (c) 2 g/l in a plating bath.

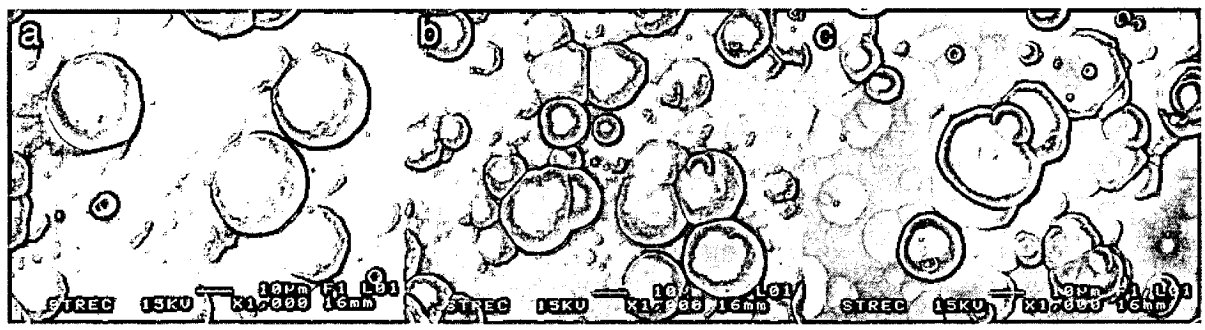

Fig. 4. Surface morphology of Ni–W/micro WC composites processed with a current density of 0.2 A/cm^2 and WC content of (a) 0.2 g/l, (b) 1 g/l, and (c) 2 g/l in a plating bath.

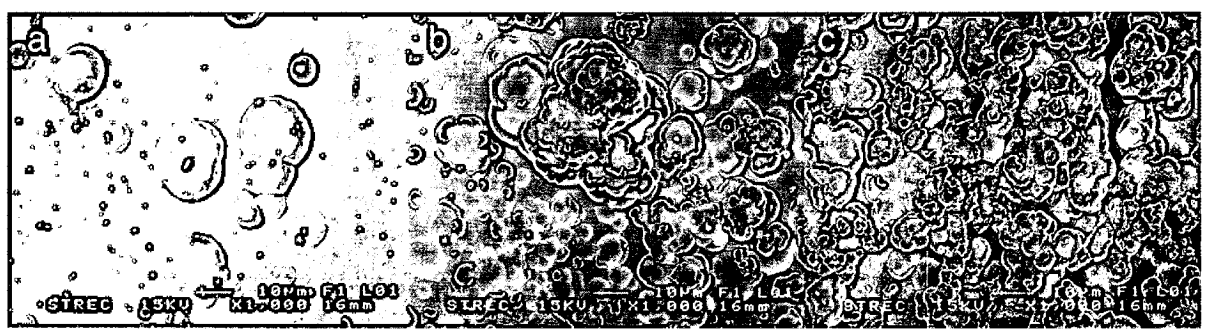

Fig. 5. Surface morphology of Ni–W/sub-micro WC composites processed with a current density of 0.1 A/cm^2 and WC content of (a) 0.2 g/l, (b) 1 g/l, and (c) 2 g/l in a plating bath.

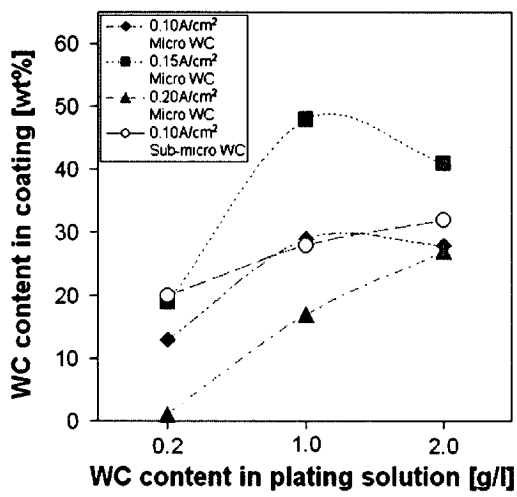

Fig. 6. The content of WC particles in Ni–W/WC composites which were fabricated using different current densities and inclusion sizes, presented as a function of WC content in a plating solution.

The chemical analyses of the surface of the as-deposited specimens, as obtained from EDS sectional area scans, reveal that the Ni–W compositions of the materials are fairly uniform in all cases, even those that exhibit nodule-matrix typed structure (Fig. 2a–c) where the chemical compositions in the nodule and matrix regions appear similar. Additionally, the relative contents of Ni and W were found to be influenced not by the content of WC incorporated, but somewhat by current density. The atomic percents of Ni–W of the deposits processed at 0.1 A/cm^2, 0.15 A/cm^2, and 0.2 A/cm^2 are respectively 75–25, 70–30, and 68–32. The X-ray diffraction patterns of the specimens with sub-micro WC, micro WC and without particle inclusions, as exemplified in Fig. 7, appear to be similar. In particular, they all exhibit broad Ni(W) peaks of comparable relative intensities showing a strong (111) texture. The results therefore suggest that nanocrystallinity and crystallographic texturing of Ni–W alloys are preserved [10], despite the inclusion of WC particles.

Fig. 8 presents the results from the hardness measurements. Without WC additions, the electrodeposited Ni–W alloys, fabricated with current densities of 0.1, 0.15, and 0.2 A/cm^2, exhibit the hardness of 2.8, 6.5 and 6.1 GPa, respectively. The incorporations of WC particles, particularly with solid loading of 1 g/l, result in a marked improvement of hardness, which is increased by a factor of up to four. At the highest

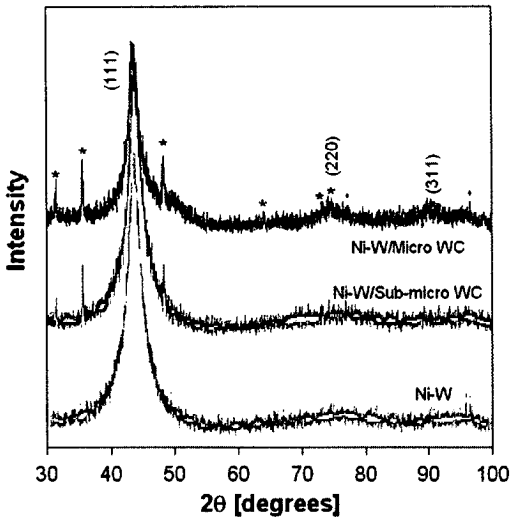

Fig. 7. X-ray diffraction (XRD) patterns of Ni–W specimens that were co-deposited with micro WC (1 g/l) and sub-micro WC particles (1 g/l), and of the specimen without WC addition. All deposits were processed with a current density of 0.1 A/cm^2. The sign * designates peaks of WC, while the indicated crystallographic planes are of Ni–W alloys.

solid loading examined (2 g/l), further increment of hardness with particle addition is observed in the 0.1 A/cm^2 specimen containing micro WC. On the other hand, the hardness of the 0.1 A/cm^2 specimen with sub-micro WC is reduced when particle addition is increased from 1 to 2 g/l. The hardness of the specimen processed at a high current density of 0.2 A/cm^2 appears not to be significantly affected by WC addition, regardless of solid loading. The deposit with 2 g/l WC processed at 0.15 A/cm^2 suffered brittle cracks upon hardness measurement, and thus its testing result is not reported in Fig. 8.

4. Discussion

4.1. Processing and microstructures

The addition of WC particles thus affects meso-scale structure of the Ni–W deposits, while grain structure and chemical composition of the alloys are undisrupted. The progress of deposits' surface morphology with modifications of current density, solid loading, and inclusion size, as described in the earlier section, may be elucidated by considering possible co-electrodeposition mechanism of the system.

On one hand, Ni and W complex ions are reduced and deposited on a substrate. In parallel, WC particles may be convectively transferred to the cathode surface and incorporated with the metal ions. It can be anticipated, therefore, that the transport rates of deposited metal ions and of particles would determine the structure of the co-electrodeposits. While the growth rate of the metal film may be controlled by the deposition current, the particle incorporation rate is influenced by the dispersion of particles, which is in turn affected by agitation of electrolyte and particles' size and concentration. Furthermore, the rate of particle incorporation can also be influenced by the growth rate of the film [20], and the cathodic current efficiency of the deposit [16].

It should be noted also that WC is thermodynamically unstable and oxidized in the presence of water or oxygen, resulting in the formation of surface oxide layers consisting mainly of WO_3 [21]. The oxide can be hydrated to give –OH group which provides a negative surface charge, which subsequently can induce absorption of Ni–W and H cations on the particles, forming surface complexes [22,23]. Consequently, incorporation of such cation-absorbed WC particles into the alloy deposits may be facilitated, and this in turn can promote reduction of H+ in the particles' area vicinity.

In the case of specimens fabricated at 0.1 A/cm^2, as shown in Fig. 2a–c, the surface morphology comprises a matrix of Ni–W and the region of Ni–W that is built up on WC agglomerates. The increase of current density to 0.15 A/cm^2 leads to the increment of metal deposition rate. This subsequently results in deposits with a turtle shell-like structure, where individual WC agglomerates are fully covered by the alloy, forming nodules (e.g., Fig. 3b). Furthermore, the enhancement of the flux of metal ions may increase the probability for particles to be entrapped in the growing film, as noted above. Indeed, it is observed that WC incorporated in the coating in the case of 0.15 A/cm^2 is higher than that with 0.1 A/cm^2. As the solid loading is increased further from 1 g/l to 2 g/l, in the vicinity of the cathode, the reduction rate of hydrogen cations absorbed on WC particles becomes significant. The release of the corresponding hydrogen atoms thus leads to a very porous structure of the deposit (Fig. 3c).

At 0.2 A/cm^2, the deposit again exhibits a turtle shell-like structure, without a clear sign of porosity (Fig. 4b and c). It can be observed from Fig. 6 that the contents of WC incorporated in the alloys processed at 0.2 A/cm^2 are relatively low, as compared to the deposits fabricated at lower current densities. This may be attributed to rapid increase of pH and hence the formation of hydrates of the metals at the cathode, for the high applied current density conditions [16]. The process can effectively lead to a reduction of the cathodic current efficiency of the deposited metals in the system, and in turn influence the incorporation rate of the particles. As shown in Ref. [4] for the Ni/SiC co-deposits, for example, while the cathodic polarization is not significantly affected by the presence of SiC particles in the bath, the cathodic current efficiency of the systems with 10 and 20 g/l SiC reaches its maximum values when the applied current density is 0.02 A/cm^2, beyond which the current efficiency drops gradually. That the content of incorporated WC particles in NiW matrix increases with current density, and decreases at high current densities, agrees well with prior studies of other co-electrodeposited systems [4,8,13,15,16].

Turning now to the cases with sub-micro particles, by comparing with the micro-particle cases (0.1 A/cm^2; 1 g/l), the structure of the deposits is filled with nodules of WC agglomerates of smaller size throughout (Fig. 5b). This should be due to better dispersion of the small WC particles in the electrolyte. When the solid content is increased to 2 g/l, the adverse hydrogen-generation effect becomes evident and contributes voids to the deposit (Fig. 5c). The voids contain sharp edges, which facilitate the formation of macrocracks as observed.

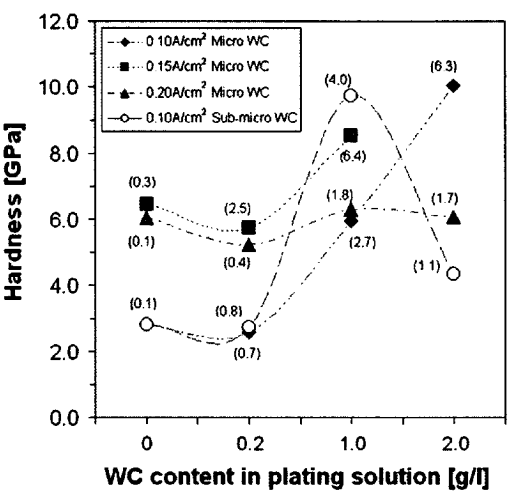

Fig. 8. The hardness of Ni–W/WC composites which were fabricated using different current densities and inclusion sizes, presented as a function of WC content in a plating solution. The standard deviations of the measurements are indicated next to the data points.

4.2. Hardness

As WC is intrinsically hard and may help impede dislocation motions in the matrix, it can be expected that incorporation of WC to Ni–W deposit may help improve mechanical properties of the alloy. The hardness of co-electrodeposited Ni–W/WC presented in Fig. 8 can stem mainly from three factors – (i) composition and grain size of Ni–W, (ii) content and distribution of WC, and (iii) microstructure as induced by WC incorporation. Without the addition of WC, the hardness of the electrodeposited Ni–W is controlled by grain size, which is in turn affected by the composition of W in the alloy [10]. Fig. 8 shows that the WC-free Ni–W deposits processed with a current density between 0.1 and 0.2 A/cm^2 exhibit the hardness between 2.8 and 6.5 GPa, in agreement with prior study [11]. The addition of WC with solid loading of merely 0.2 g/l results in moderate content of WC in the deposits with minimal influence on the underlined structure. Consequently, the hardness values of these specimens are comparable to those without WC.

The addition of WC with solid loading of 1 g/l leads to higher content of WC inclusions and modifications of the microstructure of the deposits, as discussed earlier, and these directly contribute to the increase of their hardness. Fig. 8 shows that the deposits processed with 1 g/l WC exhibit the average hardness between 5.9 and 9.7 GPa, depending on current density used. The deviations of hardness from the average values, however, are large in these specimens. With higher content of WC addition and better particle de-agglomeration, such variation may be lessened. When the solid loading is increased to 2 g/l, porosity was induced in some deposits (micro WC, 0.15 A/cm^2; sub-micro WC, 0.1 A/cm^2), and this results in degradation of hardness and facilitates the formation of brittle cracks as expected.

Of all deposits investigated, that processed with 1 g/l sub-micro WC, which exhibits a dense nodular agglomerate structure (Fig. 5b), shows the most significant hardness enhancement. In particular, its average hardness of about 10 GPa is comparable to that of the hard chromium coatings. On the other hand, with small content of WC inclusions, the hardness of the composites processed with a current density of 0.2 A/cm^2 is relatively low.

5. Conclusion

The present study has therefore shown that WC can be co-electrodeposited with nanocrystalline Ni–W alloys, and that (i) current density, (ii) solid loading, and (iii) particle size are all important processing parameters that control the microstructure, the content of WC incorporated and hence the apparent hardness of the composite. This is attributed to the influence of these parameters on the transport rates of the plating metals and of the particles, and the generation of hydrogen in the deposition baths. The WC content in the Ni–W deposits generally increases with WC content in the electrolyte, and also with current density up to 0.15 A/cm^2, beyond which decrement of WC content occurs. Moderately-high current density and solid loading (~0.15 A/cm^2 and 1–2 g/l, respectively) are found essential in providing deposits with non-porous and uniform structure. Furthermore, reduction of the particle size of WC further benefits the dispersion of WC in the deposit, resulting in high hardness which surpasses that of Ni–W alloys and at par with that of hard chromium coatings. The degree of particle dispersion may be enhanced further by adding surfactants in a plating bath or applying ultrasonic energy upon deposition, and this would lead to a more homogeneous surface morphology and higher content of particles incorporated.

Acknowledgement

YB gratefully acknowledges Prof. C.A. Schuh of Massachusetts Institute of Technology for useful discussions and supports. The Thailand Research Fund financially supported this work under contract TRG5180008; the sponsor does not endorse the views presented herein.

References

[1] C.T.A. Low, R.G.A. Wills, F.C. Walsh, Surf. Coat. Technol. 201 (2006) 371.
[2] Q. Feng, T. Li, H. Teng, X. Zhang, Y. Zhang, C. Liu, J. Jin, Surf. Coat. Technol. 202 (2008) 4137.
[3] J. Steinbach, H. Ferkel, Scripta Mater. 44 (2001) 1813.
[4] L. Burzynska, E. Rudnik, J. Koza, L. Blaz, W. Szymanski, Surf. Coat. Technol. 202 (2008) 2545.
[5] P. Gyftou, E.A. Pavlatou, N. Spyrellis, Appl. Surf. Sci. 254 (2008) 5910.
[6] F. Wuensche, A. Bund, W. Plieth, J. Solid State Electrochem. 8 (3) (2004) 209.
[7] A. Lozano-Morales, E.J. Podlaha, J. Electrochem. Soc. 151 (7) (2004) C478.
[8] Y.L. Wang, Y.Z. Wan, S.M. Zhao, H.M. Tao, X.H. Dong, Surf. Coat. Technol. 106 (1998) 162.
[9] Y.L. Yang, Y.D. Wang, Y. Ren, C.S. He, et al., Mater. Lett. 62 (2008) 47.
[10] A.J. Detor, C.A. Schuh, Acta Mater. 55 (2007) 371.
[11] C.A. Schuh, T.G. Nieh, H. Iwasaki, Acta Mater. 51 (2003) 431.
[12] C. Bergenstof Nielsen, P. Leisner, A. Horsewell, J. Appl. Electrochem. 28 (1998) 141.
[13] B. Han, X. Lu, Surf. Coat. Technol. 202 (2008) 3251.
[14] Y. Yao, S. Yao, L. Zhang, H. Wang, Mater. Lett. 61 (2007) 67.
[15] L. Shi, C. Sun, P. Gao, F. Zhou, W. Liu, Appl. Surf. Sci. 252 (2006) 3591.
[16] Z. Abdel Hamid, I.M. Ghayad, K.M. Ibrahim, Surf. Interface Anal. 37 (2005) 573.
[17] K. Van Acker, D. Vanhoyweghen, R. Persoons, J. Vangrunderbeek, Wear 258 (2005) 194.
[18] B.Y.C. Wu, P.J. Ferreira, C.A. Schuh, T.G. Nieh, Metall. Mater. Trans. A 36A (2005) 1927.
[19] S. Ruan, C.A. Schuh, Scripta Mater. 59 (11) (2008) 1218.
[20] P.M. Vereecken, I. Shao, P.C. Searson, J. Electrochem. Soc. 147 (7) (2000) 2572.
[21] L.M. Andersson, L. Bergstrom, Int. J. Refract. Met. 18 (2000) 121.
[22] L.E. Lynn, K.F. Hayes, J. Colloid Interface Sci. 170 (1995) 477.
[23] M. Stroumbouli, P. Gyftou, E.A. Pavlatou, N. Spyrellis, Surf. Coat. Technol. 195 (2005) 325.